



TECHNICAL ARTICLE

Comparison of Three-Body Abrasion Behaviors of High-Cr-Mo- and High-Cr-Based Multicomponent White Cast Irons

Riki Hendra Purba, Kazumichi Shimizu, Kenta Kusumoto, and Yila Gaqi

Submitted: 24 March 2022 / Revised: 30 June 2022 / Accepted: 30 July 2022 / Published online: 21 September 2022

The effect of molybdenum (0-3 wt.% Mo) on three-body abrasive wear characteristics of high-chromium (16 and 26 wt.% Cr) white cast iron has been evaluated in the current study and compared with high-Cr-based (18 and 27 wt.%) multicomponent (3 wt.% of each Mo, vanadium, tungsten, and cobalt) white cast iron (MWCI). Results show Mo and Cr can increase hardness and wear resistance of high-Cr white cast iron, although the opposite occurs when Mo addition exceeds 1% wt. in the case of 26Cr because of lowering carbide volume fraction. In addition, the wear rate of 26Cr-1Mo is 53% higher than 18Cr MWCI, whereas it is only less than 15% compared with 27Cr MWCI. The lowering C concentration in the matrix as Cr increases must be a factor of wear resistance reduction in the case of high-Cr MWCI. Therefore, the abrasive wear of materials strongly depends on chemical composition, matrix, and carbide volume fraction.

Keywords abrasive, chromium, molybdenum, multicomponent

1. Introduction

Abrasive wear is a type of material failure due to the removal and deformation of the material's surface because of the mechanical action of the contacting object through relative motion (Ref 1). It has been reported that besides annually producing 970 million tons of CO₂ emissions, wear phenomenon can consume a large of gross national product, which abrasive wear phenomenon can spend approximately 1.4% (Ref 2). It has been estimated that there are approximately \$68 billion economic losses every year owing to replacement of wear machine parts in the mineral mining factory (Ref 3). Therefore, superior wear-resistant materials are still in great demand today.

High-chromium (Cr) white cast iron (HCCI) has been broadly applied on wear conditions due to the precipitation of hard phase such as M₃C (840-1240 HV), M₇C₃ (1000-1800 HV), and M₂₃C₆ (1000 HV) carbide. The letter M is mostly occupied by the Cr, and the stoichiometry of carbide strongly depends on the chemical composition of materials. From many studies, it can be concluded that HCCI containing more carbide volume fraction (CVF) of M₇C₃ has better wear

resistance owing to higher hardness value than other types (Ref 4-9). However, the existence of this hard carbide on the microstructure produces a brittle HCCI, resulting in limited application. Various methods have been diligently conducted by many scholars to develop the wear resistance of HCCI. Since a long time ago, it has been known that by transforming the austenite matrix to martensite during the heat treatment process, a higher matrix hardness can be achieved. Therefore, once the abrasive particles hit the material surface, the martensite can stand firmly and reduce the crack possibility of M₇C₃ that significantly improves the wear resistance of HCCI (Ref 10, 11). Besides that, it has been known that Cr will react with the adjacent carbon on the matrix area to form a fine secondary carbide during destabilization heat treatment, which can effectively reinforce the matrix of material leading to better wear resistance (Ref 12, 13). Coronado (Ref 14) proposed another effort by modifying the M₇C₃ carbide orientation to achieve higher-toughness carbide without changing the carbide type via adjusting the cooling rate of iron molten during the solidification process. The addition of other stronger transition metals, such as titanium, niobium, vanadium, tungsten, and molybdenum (Mo), can be also an alternative way to get a better wear resistance of HCCI (Ref 14-20). It is well known that apart from titanium, niobium, and vanadium will precipitate as MC carbide; it also effectively refines the size of M₇C₃ carbide because of its inoculant characteristics, which provide better wear resistance. However, Ibrahim et al. (Ref 21) stated that the reverse result must occur if the amount of these elements is excessive because of the clustering effect on the matrix. Meanwhile, Mo and tungsten can increase the hardenability and act as carbide-forming elements, which can significantly improve the wear resistance of HCCI (Ref 22-25). In particular, Inthidech et al. (Ref 22) concluded that Mo can increase the wear resistance of hypoeutectic 16 wt.% Cr white cast iron under two-body abrasion owing to higher hardness. However, Shimizu et al. (Ref 23) revealed that there is no different erosive wear resistance between 26 and 16 wt.%

Riki Hendra Purba, Production System and Engineering, Muroran Institute of Technology, Muroran City, Hokkaido, Japan; and Mechanical Engineering Department, University of Sumatera Utara, Medan, Indonesia; and **Kazumichi Shimizu**, **Kenta Kusumoto**, and **Yila Gaqi**, Production System and Engineering, Muroran Institute of Technology, Muroran City, Hokkaido, Japan. Contact e-mails: 20096010@mmm.muroran-it.ac.jp, Rikipurba@gmail.com, and kusumoto@mmm.muroran-it.ac.jp.

Cr with the same amount of Mo (3 wt.%) at high temperature because of a higher Mo₂C CVF of 16Cr-3Mo than 26Cr-3Mo. It means that the performance of this material strongly depends on the wear condition. Thus, it is important to investigate the wear characteristics of these HCCIs under abrasion conditions, which is the biggest contributor of mechanical failure due to wear as described previously to enrich the theoretical understanding of the three-body abrasive wear phenomenon.

Because the above transition metals can solidify as extremely hard carbides, several of them have been added to white cast iron named multicomponent white cast iron (MWCI) recently. It can be applied in many machines parts, especially on roll-mill and pulverizing equipment. The better wear resistance materials can be obtained because of more variations of carbide on microstructure compared with HCCI (Ref 26-28). The effect of cobalt (Co) on the high-temperature erosive wear test of the multicomponent white cast also has been investigated. Kusumoto et al. (Ref 29) have revealed that Co can strengthen the matrix, although its nature is not a carbide-forming element. However, once the amount of Co is over the threshold (> 5 wt.%), the wear resistance of this material will actually decrease owing to lowering hardness. Most lately, we have evaluated the erosive wear performance of high-Cr-based (18 and 27% wt.) MWCI (3% wt. each of V, Mo, W, and Co) with three conditions: as-cast, quenched, and quenched-tempered. The result shows that 18Cr MWCI or 27Cr MWCI after quenching is better than other conditions (as-cast and quenched-tempered) due to good synergy between matrix and carbides (Ref 30). However, there seems a new problem due to superhigh production costs compared with traditional HCCI with Mo addition. Therefore, besides evaluating the three-body abrasive wear behavior of high-Cr-Mo white cast irons, it would be also compared with two high-Cr MWCI after the destabilization heat treatment process in this study to determine the life span of each material.

2. Methodology

2.1 Material Preparation

In this present study, 16 and 26 wt.% Cr with 0-3 wt.% Mo in the case of high-Cr-Mo white cast iron and 18-27 wt.% Cr-based 3 wt.% (V, Mo, W, and Co) for high-Cr MWCI were added. The manufacturing process has been described in our previous study (Ref 9). It can be highlighted briefly as first 50 kg of raw materials were melted using a high-induction furnace and poured into Y sand mold. Second, each material was cut with 50 × 50 × 10 mm using a high-speed precision cutting machine (RCA-234; Refinotech Co, Ltd, Japan). Material composition was measured using SPECTROLAB (AMATEK, Inc, America) as provided in Table 1. Scanning electron microscopy (SEM) and energy-dispersive x-ray spectroscopy (EDS) (with type JXA-9800 R, Japan) was used to analyze the microstructure before and after etching in 5% nitrohydrochloric acid. ImageJ was utilized to calculate the CVF. A grinder machine was utilized to clean each material surface (GS52PF; Kuroda Seiko Co, Ltd).

Generally, HCCI will be quenched after heating with a temperature range of 1173-1423 K for quenching followed by tempering after heating 693-813 K to transform the austenite to martensite and precipitate the secondary carbide (Ref 11-13, 31,

Table 1 Chemical composition of materials

Materials	C	Cr	Mo	W	V	Co	Fe
16Cr	2.86	15.75	0.15	Bal.
16Cr-1Mo	2.83	16.03	1.04	Bal.
16Cr-3Mo	2.71	16.05	3.07	Bal.
26Cr	2.84	25.65	0.05	Bal.
26Cr-1Mo	2.79	25.81	0.96	Bal.
26Cr-3Mo	2.87	25.68	2.86	Bal.
18Cr-MWCI	2.91	17.01	2.84	2.61	2.85	2.71	Bal.
27Cr-MWCI	2.93	26.59	2.64	2.78	2.93	2.62	Bal.

32). Some published articles revealed that the increasing hardness of materials will provide better wear resistance, although the toughness should be controlled in certain cases by keeping a small amount of austenite in the microstructure after heat treatment (Ref 11, 33). Therefore, only the hardest materials would be chosen that might have the lowest amount of retained austenite (RA) in the microstructure after destabilization heat treatment within that temperature range. Meanwhile, the effect of heat treatment temperature on the wear performance of materials can be used as the next research topic. Based on this reason, it has been quenched by air force cooling after heating at 1323 K for 2 h and then tempered at 723 K (26Cr), 748 K (16Cr, 26Cr-1Mo, and 26Cr-3Mo), 798 K (16Cr-1Mo), and 823 K (16Cr-3Mo) (Ref 22, 34). Meanwhile, high-Cr MWCI would be quenched after heating to both 1273 K (18Cr MWCI) and 1323 K (27Cr MWCI) for 1 h without the following tempering due to the best erosive wear resistance materials in our previous study (Ref 30). In addition, the different chemical compositions of each material might influence the microstructure constituents of materials, for instance, CVF, carbon solubility on matrix, and the percentage of RA. Thus, it might also give different temperatures of heat treatment that has the higher hardness of each selected material in this study. X-ray diffraction (Ultima IV, Rigaku, Japan, with Cu-K α source) was used to identify the phase of materials microstructure. The volume fraction of RA (f_{RA}) was calculated using the following formula:

$$f_{RA} = \frac{100\%}{1 + G\left(\frac{I_x}{I_\gamma}\right)} \quad (\text{Eq 1})$$

where I_x and I_γ are the peak intensity of α -Fe (200), (211) and γ -Fe (200), (220), (311), and G is coefficient corresponding to the different combination as proposed in (Ref 35).

2.2 Three-Body Abrasive Wear Testing

A rubber wheel three-body abrasive wear machine according to ASTM G65 was used to evaluate the abrasion characteristic of the material at 73.5-, 145-, and 196-N load. Total sliding distance is approximately 430 m, and sliding speed is 1.2 m/s. Silica sand was used as an abrasive particle with 1100 HV1 hardness and 300 μ m in size. The machine test and the silica sand are provided in Fig. 1(a), (b) and (c). Every test was repeated six times, and the average obtained results were used. To calculate the wear rate of each material, the following equation was used:

$$\text{Wear rate} = \frac{\Delta m}{\pi d t n} \quad (\text{Eq 2})$$

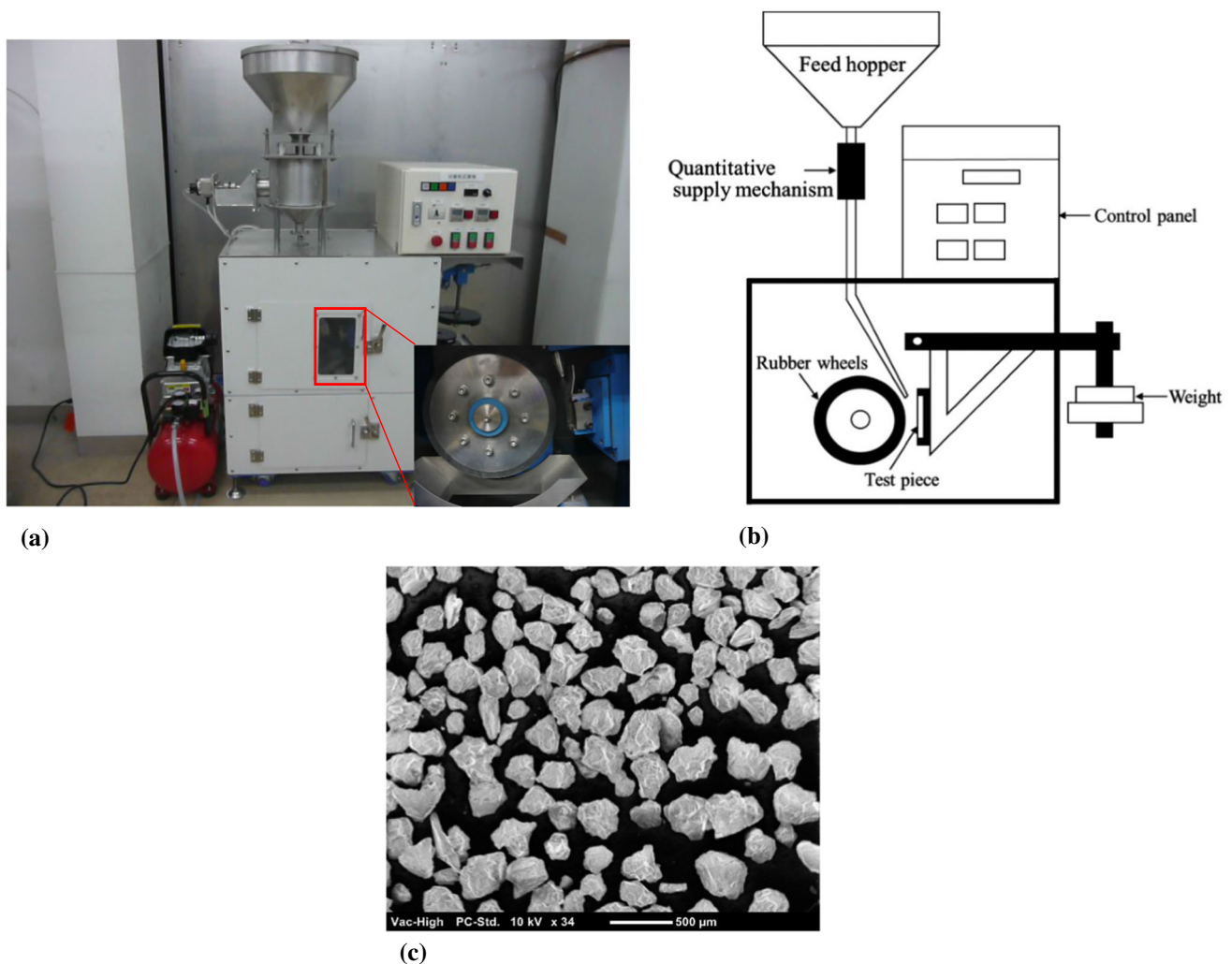


Fig. 1 (a) The three-body abrasion machine test according to ASTM G65; (b) Schematic of abrasive wear machine; (c) Abrasive particles

where Δm is material weight loss; d is the diameter of the wheel; t is time; and n is rotating speed.

2.3 Vickers Hardness Test

In this present study, there are two hardness data provided. Microhardness and macrohardness were measured using FV-800 and FM-300 (Future-Tech Co, Ltd; Japan). The macrohardness indicates the entire material hardness (matrix plus carbide), whereas microhardness is the matrix.

3. Results and Discussion

3.1 Materials Microstructure Observation

The microstructure of materials is an important factor to evaluate the wear characteristic of a material, especially HCCI. Therefore, the microstructure of each test piece was investigated using the optical microscope after etching on 5% nitrohydrochloric acid for 4-6 min. The microstructure of representative materials is shown in Fig. 2. It can be seen that there are plenty of precipitated carbides on the microstructure, which is well distributed in a long matrix area as pointed out in

the figure. It informs that the primary eutectic carbide (hexagonal one) is getting bigger as the amount of Cr addition increases in the case of high-Cr MWCI. In several previous studies (Ref 36-39), it has been reported that M_7C_3 carbide has a hexagonal Bravais lattice because of its hexagonal shape, although in certain cases, it can be an orthogonal crystal structure. To provide more accurate data, a depth etching with 5% nitrohydrochloric liquid was carried out on representative materials for 1 week as shown in Fig. 3. The result is shown in the figure, the relatively similar shape of M_7C_3 as also observed as hexagonal rods in a previous study. Therefore, it can be assumed that primary M_7C_3 carbide in this study has Bravais lattice structure. The average size of primary M_7C_3 carbide increased from approximately $28 \pm 1.55 \mu\text{m}$ (18Cr MWCI) to $44 \pm 4.2 \mu\text{m}$ (27Cr MWCI) obtained using the binarizing technique in the ImageJ software. Because the Cr is a strong carbide-forming element, the higher amount of Cr addition will naturally segregate the more C atom in iron molten, and it will also occupy more the stoichiometry of M_7C_3 that might effectively enlarge the size of this carbide. Meanwhile, although carbide precipitation of 26Cr (size of M_7C_3 approximately $26 \pm 3.7 \mu\text{m}$) seems to be more densely distributed than 18Cr MWCI, no significant difference in dimensions of the primary M_7C_3 carbide is observed, which is elusive these

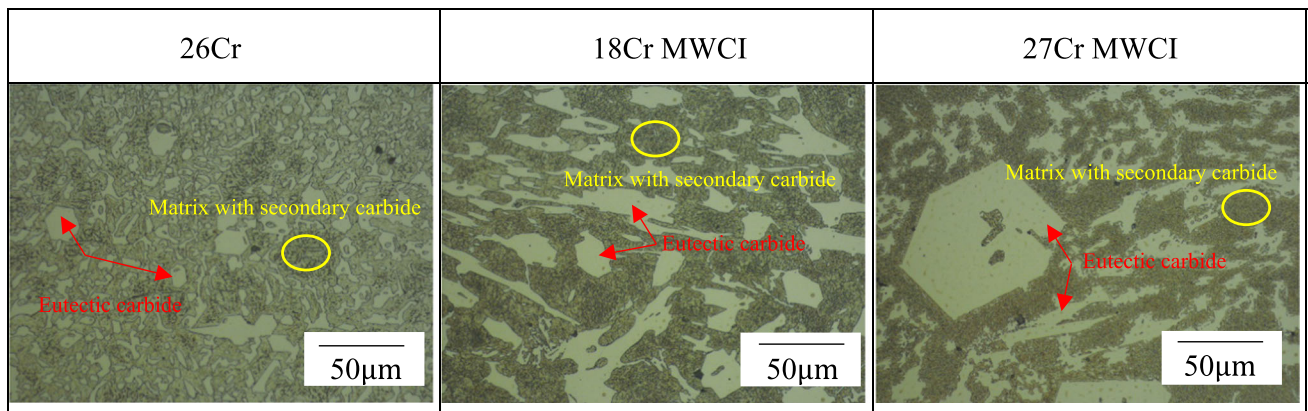


Fig. 2 Microstructure of materials observation using optical microscope after etching with 5% nitro hydrochloric acid

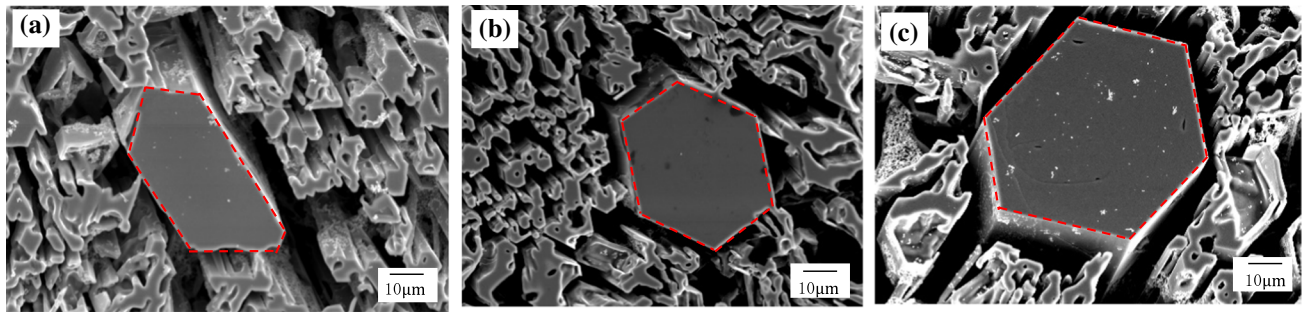


Fig. 3 Hexagonal rod shape of primary M_7C_3 carbide on: (a) 26Cr-3Mo; (b) 18Cr MWCI; and (c) 27Cr MWCI after deep etching

results from this point of view. In addition, the distribution of each added transition metal on the microstructure is also difficult to determine. Therefore, the investigation was continued using SEM-EDS, and the results are given in Fig. 4.

From the microphotograph of the SEM-EDS image, it can be seen that black carbide is mostly occupied by Cr in the case of high-Cr-Mo specimens. The stoichiometry of this carbide is M_7C_3 obtained by point analysis at more than 10 different SEM-EDS locations. Meanwhile, deposition of M_2C (the letter M is occupied by Mo) carbide can only be observed at 16Cr-3Mo and 26Cr-3Mo. Also, it shows that the volume fraction of M_7C_3 carbide seems to decrease on 3 wt.% Mo addition on either 16Cr or 26Cr. It can be understood that Mo atom will be stronger to form carbides than Cr atom because of its higher mixing enthalpy (Ref 40). Thus, once temperature of melt and the percentage of Mo are sufficient to form M_2C carbides (in this case, approximately 3 wt.%), it will deplete the available C content for Cr atom, which in turn reduces the CVF of M_7C_3 . The CVF of each material would be measured to prevent speculation as given in the bar chart of Fig. 5. However, before explaining the results, it can also be observed that the M_7C_3 of high-Cr MWCI is occupied by V elements other than Cr, Fe, and C. This must be a contributing factor to the size of the M_7C_3 carbide on 18Cr MWCI being comparable to 26Cr despite having a lower amount of Cr addition as previously described. Meanwhile, M_2C carbide of the two high-Cr MWCI is simultaneously occupied by W and Mo. With a higher magnification as shown in Fig. 6, the needle-like matrix informs that martensite (α') is the main matrix in addition to secondary carbide deposition ($M_{23}C_6$) and a small amount of RA. From x-ray diffraction data as shown in Fig. 7, it is known

that RA percentage of 16Cr with 0-3 wt.% Mo is approximately 4-11, and that of 26Cr with 0-3 wt.% Mo is approximately 2-8. However, the RA is difficult to observe in the case of high MWCI. Because the only hardest material was chosen after cooling (heat temperature range, 1173-1423 K) in the case of high MWCI, the amount of RA might be too small. There is also only martensite detected by XRD, whereas RA is difficult to be found in the case of high-Cr MWCI, which can support the earlier argument. In addition, plural types of carbides can be indexed on all specimens' microstructure. It is definitely due to the high affinity of C to transition metals.

Figure 5 shows that total CVF increases as Cr increases in all materials. It is also increased by the precipitation of M_2C carbide in the microstructure of 16Cr. However, a reverse trend occurs in the case of 26Cr, which is decreased as the precipitation of M_2C carbide. In addition, the CVF of M_2C carbide in the microstructure of 26Cr-3Mo is lower than that in 16Cr-3Mo. It is understood that the higher amount of Cr will consume more C solubility to form more M_7C_3 carbides. Besides that, it is known that M_7C_3 carbide will firstly precipitate, and then, followed by the formation of M_2C carbide in the high Cr-Mo white cast iron solidification system. Thus, the higher amount of Cr addition will leave lower the C solubility for Mo to form M_2C once the iron melt is reaching the temperature its formation. This phenomenon might cause the 26Cr-3Mo is lower CVF of M_2C than 16Cr-3Mo. In addition, the M_2C of 18-27Cr MWCI is higher than high-Cr-Mo materials, which must be caused by simultaneously dissolved W and Mo. However, it is not different between both comparable materials owing to the same addition of W and Mo. The CVF M_7C_3 is getting higher as the amount of Cr

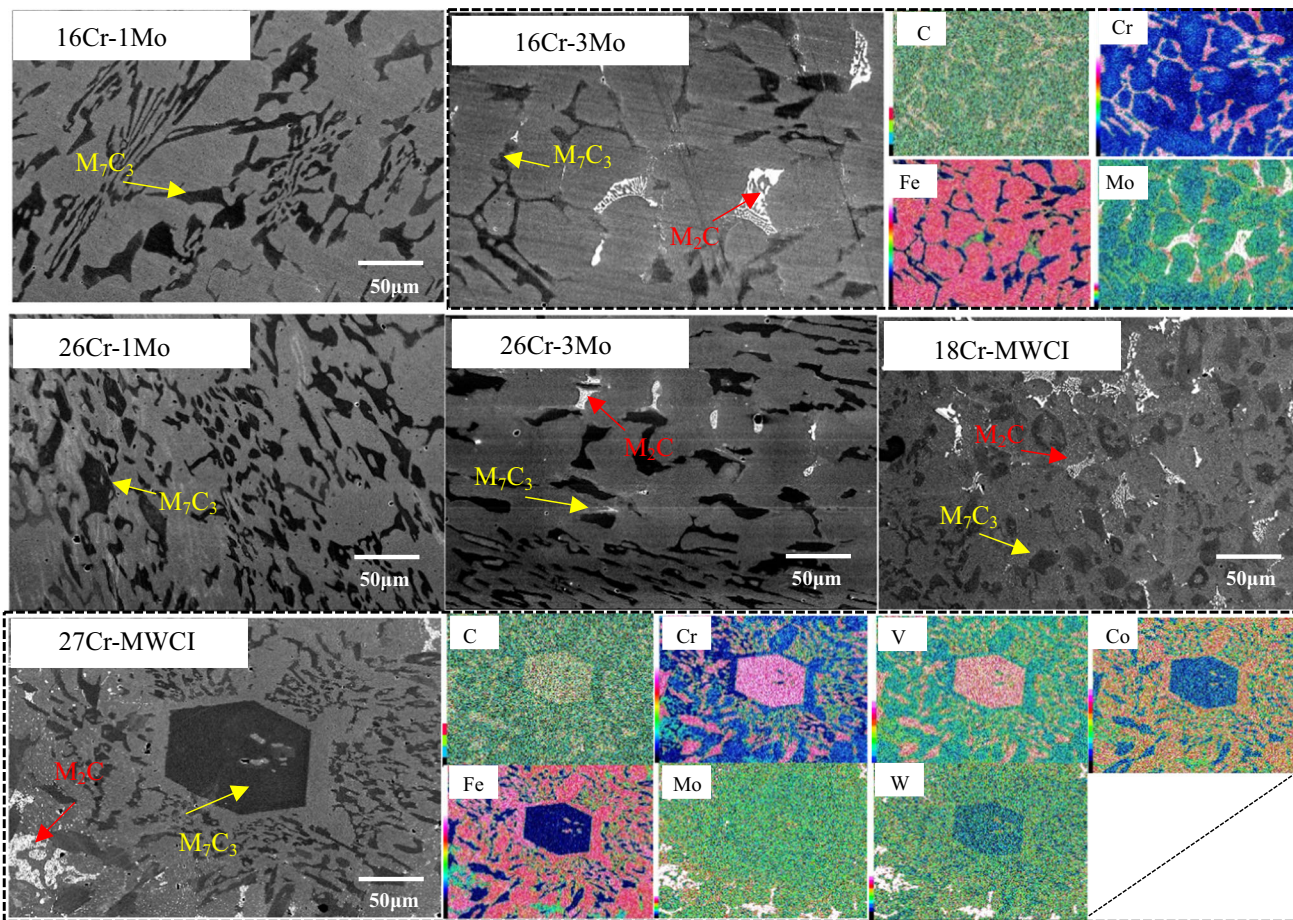


Fig. 4 SEM-EDS microphotograph of materials

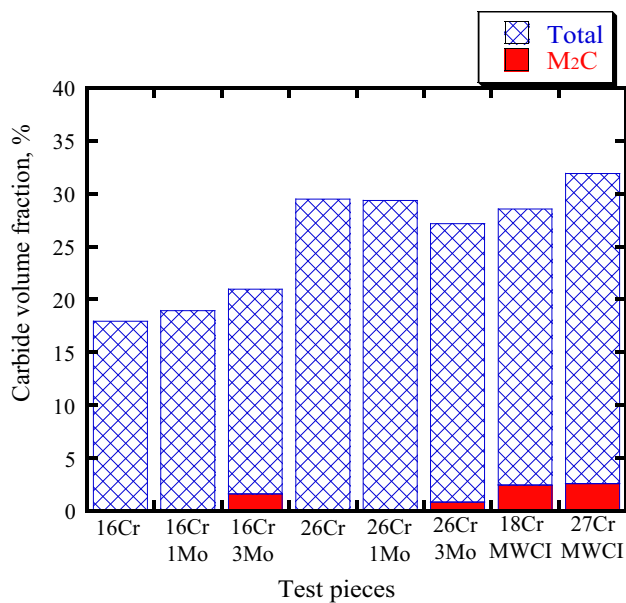


Fig. 5 The carbide volume fraction (CVF) percentage of each tested material

increases in the case of high-Cr MWCI. Therefore, it can be said that the ability of transition metals to form carbide depends not only on the higher mixing enthalpy but also on the overall

chemical compound and the available C solubility. These microstructure conditions would be attributed to the hardness and abrasive performance of materials.

3.2 Vickers Hardness Data of Each Material

Figure 8 shows the microhardness (matrix only) and macrohardness (matrix plus carbide) of each material, which is obtained by 12 times repetition test. The hardness of 16Cr white cast irons increases as the amount of Mo increases. The hardness also increases as the amount of Cr addition increases when comparing both high-Cr-Mo materials at the same Mo addition. It might be associated with the higher total CVF and a lower percentage of RA as expected. However, the hardness of the material is not consistent with the CVF in the case of 26Cr. It can be seen that the hardness of the material slightly increases as the amount of Mo increases, although the CVF is getting lower after adding 3 wt.% Cr and has relatively comparable RA with each other. It must be caused by the precipitation of M₂C carbide in the microstructure of 26Cr-3Mo as described earlier. From this result, it can be said that a higher CVF of material will not always guarantee better hardness.

In the case of both high-Cr MWCI, the hardness of the material is getting lower as the amount of Cr increases despite having CVF. This finding is different from the case of both high-Cr-Mo specimens. The depletion of C solubility on the matrix owing to the excessive addition of Cr as explained in the previous section must be the factor of this result. In addition,

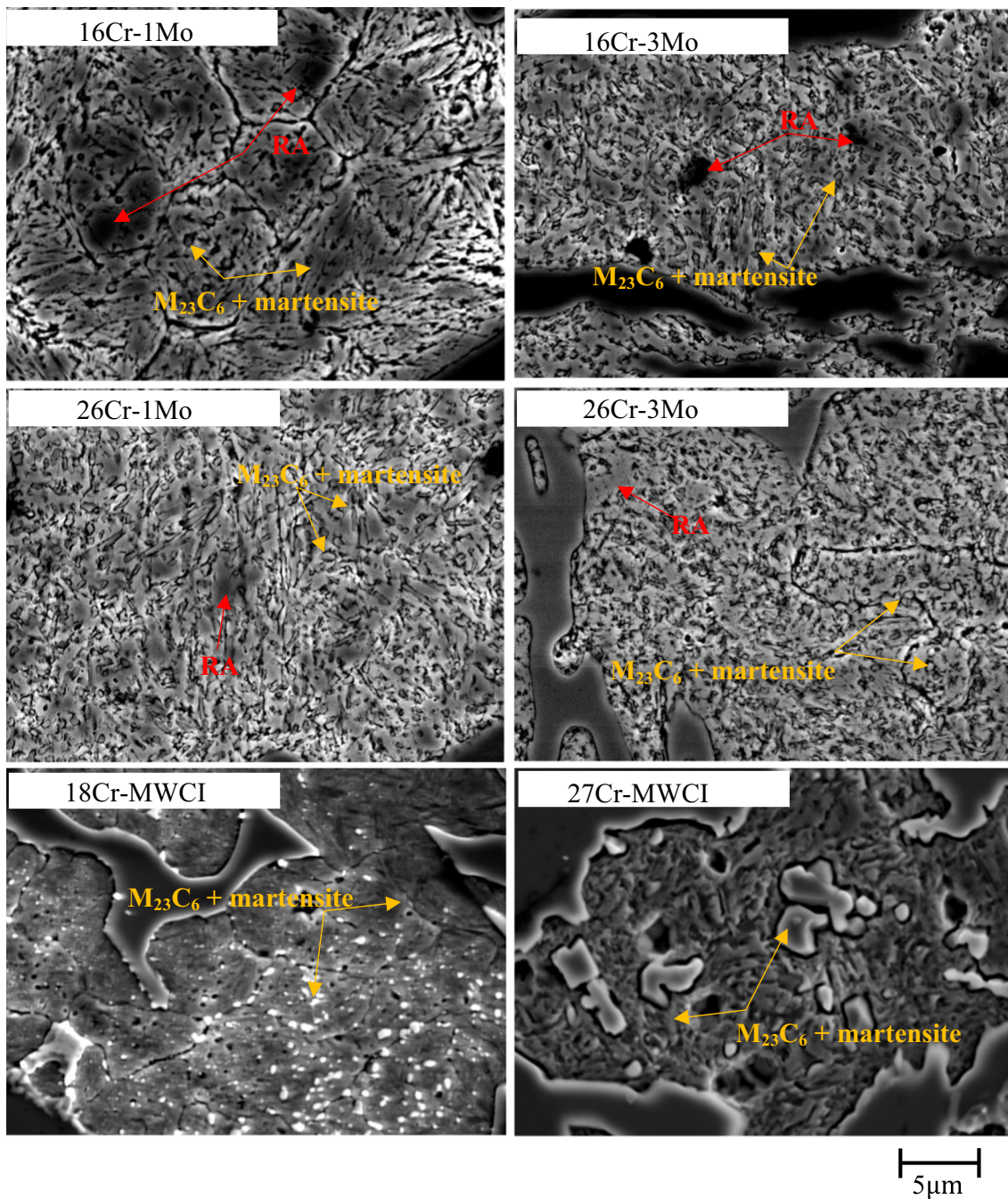


Fig. 6 Secondary carbide and matrix type of test piece after etching with 5% nitro hydrochloric acid

the hardness of both high-Cr MWCI is higher compared with high Cr-Mo. It must be caused by the different destabilization heat treatment processes. The high-Cr MWCI have quenched martensite matrix, whereas high-Cr-Mo specimens have the quenched-tempered one. Besides that, the higher CVF of high-Cr MWCI than high Cr-Mo can be also attributed to the significant improvement in material hardness. Therefore, it can be stated that the hardness of materials must strongly depend on the overall chemical composition and the heat treatment condition. From this result, it can be known that the lowest microhardness and macrohardness belong to 16Cr (494 HV0.1 and 746 HV30), whereas the highest one is 18Cr MWCI (720 HV0.1 and 983 HV30), respectively. In addition, it can be

known that martensite (300-900 HV) is mainly matrix type from microhardness data, which are in well agreement with the SEM-EDS and XRD results (Ref 38).

3.3 Three-Body Abrasive Behavior of Each Material

According to many previous studies (Ref 39, 41), the abrasive wear rate of HCCI addition increases as the number of the applied load increases. However, the abrasive wear behavior of high-Cr-based MWCI is not reported yet. Therefore, the pre-experiments were carried out on both high-Cr MWCI at 73.5-, 145-, and 196-N applied loads. The average result (Fig. 9) was obtained from three repetition tests, and the scatter bars show the standard deviation. Both materials also

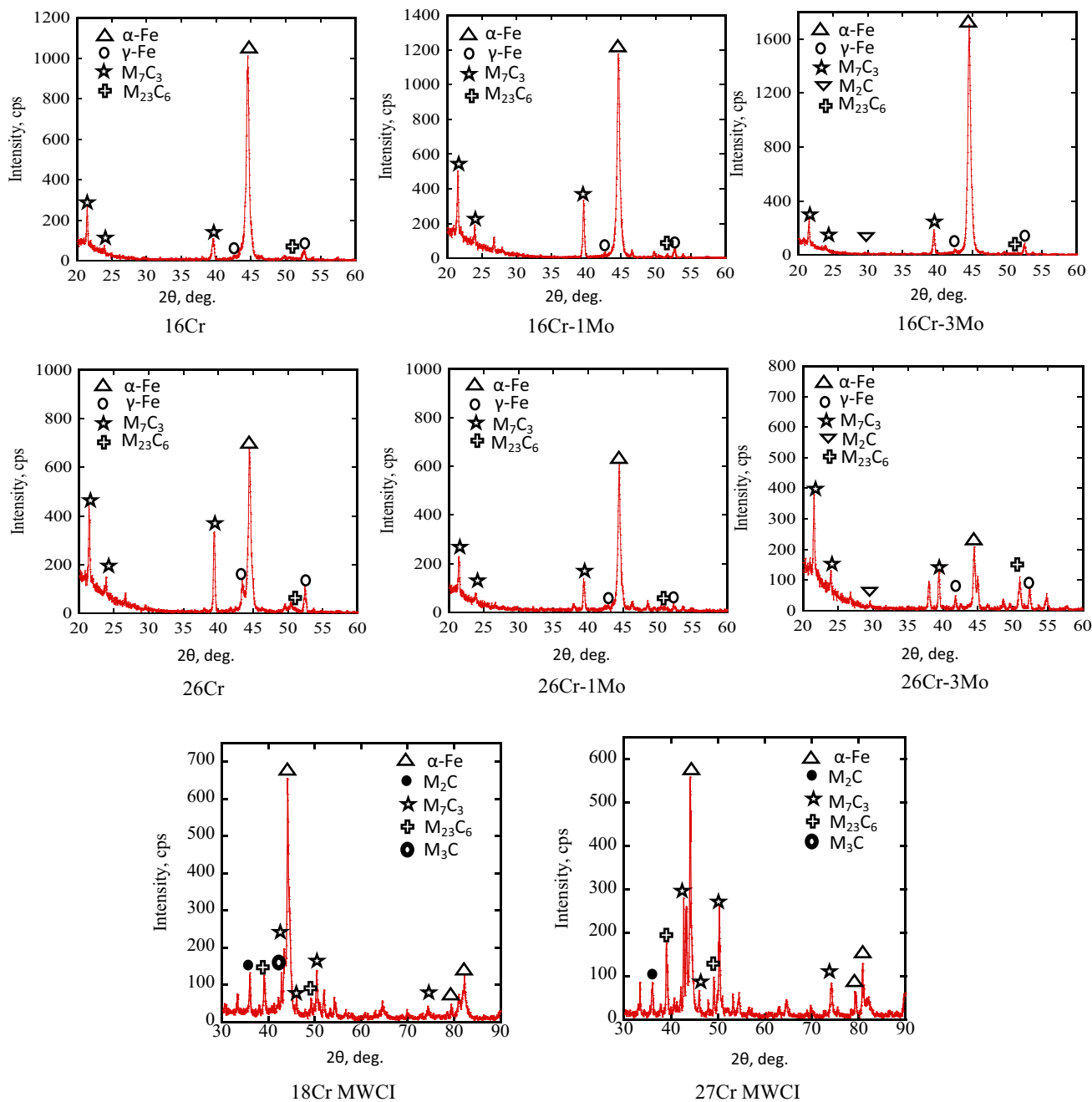


Fig. 7 X-ray diffraction of each materials

have the same tendency as HCCI, in which the heavier load has a higher amount of material loss. In order to get closer data to real engineering field, the comparison wear resistance would be focused on the highest applied load (196 N).

Figure 10 shows that abrasive wear rate is decreased as Mo increases in the case of 16Cr. It might be caused by the higher hardness as described earlier. And the result shows that wear resistance of 26Cr with the same amount of Mo addition is higher than that of 16Cr, which might be also associated with its higher CVF and higher hardness. Meanwhile, the abrasive wear resistance of 26Cr is first increased after adding 1 wt.% Mo, and then it is decreased as the amount of Mo increased up to 3 wt.% despite having higher hardness. This fact might be caused by the lowering M_7C_3 CVF after 3 wt.% Mo resulting

26Cr-1Mo has better abrasive wear resistance among high-Cr MWCI materials (approximately 0.8175×10^{-4} g/m). Therefore, it can be said that the hardness of the material cannot always be a good indicator to evaluate the wear behavior of materials.

In the case of both high-Cr MWCI, the wear resistance of materials decreases as the amount of Cr increases. This performance is totally different with two high-Cr-Mo white cast irons. It can be understood that the higher amount of Cr addition will bind more C atom to form more CVF during solidification. Thus, it would deplete C concentration in the matrix, which can be evidenced by the lower microhardness (matrix hardness) as the amount of Cr increases. Eventually, the wear resistance of 18Cr MWCI is higher than that of 27Cr

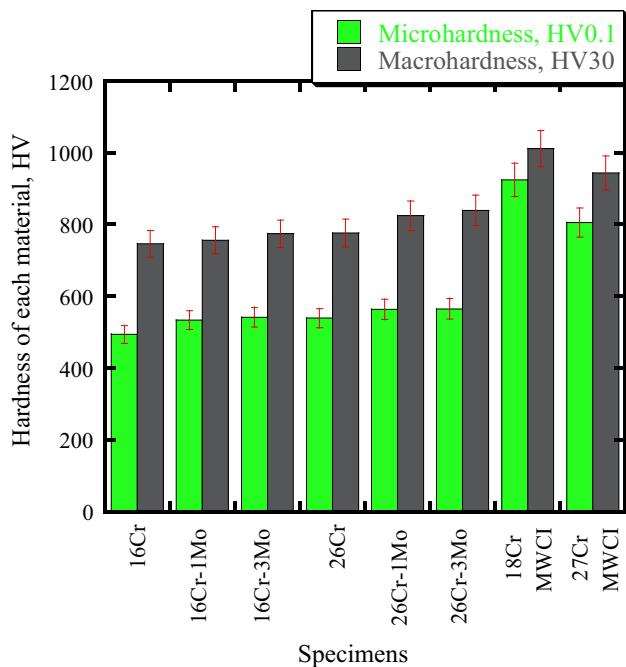


Fig. 8 Vickers hardness value of every tested material

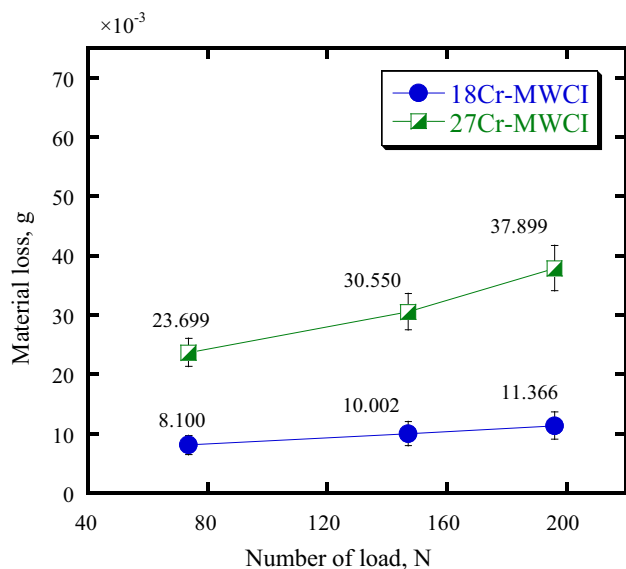


Fig. 9 Amount of materials loss as a function of applied loads

MWCI. In addition, when comparing with the best wear resistance materials among high-Cr-Mo white cast iron specimens, the abrasion rate of 26Cr-1Mo is 53% higher than 18Cr MWCI, but it is only 15% higher than 27Cr MWCI. Therefore, it can be stated that the wear characteristic of each material depends on chemical composition and microstructure constituents (CVF and matrix hardness). To provide more com-

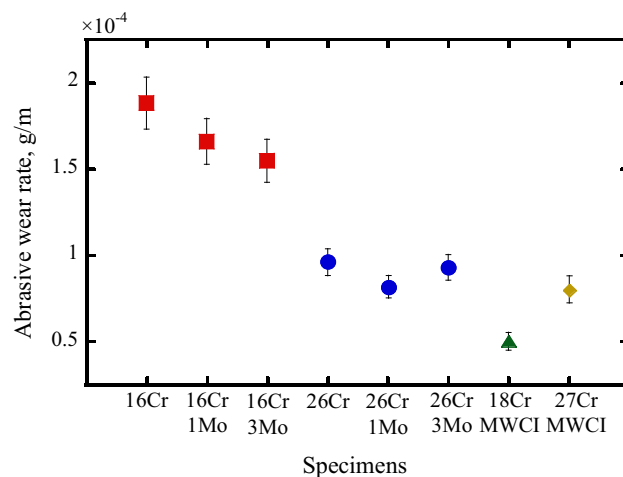


Fig. 10 Abrasive wear rate of each material with 196 N applied load

prehensive theoretical knowledge, the abrasive wear mechanism would also be investigated in this present study.

3.4 Three-Body Abrasive Wear Mechanism of Each Material

In gaining a detailed explanation, the abrasive mechanism would be also investigated through a microphotograph of the most abraded surface (Fig. 11). The sign of the microcutting in the matrix area that might be caused by lower hardness than the abrasive particle (1100 HV1) can be seen. However, the existence of microcutting cannot be clearly observed in the 18Cr MWCI material, which can be ascertained because of its high hardness. The micropitting also appears mostly in the M_7C_3 carbide, but it seems more resistant than the matrix. The M_7C_3 carbide of 27Cr MWCI seems directly peeling out. In the previous study (Ref 30), it has been reported that the larger M_7C_3 carbide is prone to peeling out directly because of its brittleness characteristics or lower fracture toughness. It means this condition must also be the factor in making the wear resistance of 27Cr MWCI not significantly higher than that of 26Cr-1Mo in addition to lower matrix hardness. It can be understood that particles would mostly scrap the matrix and slip away from the carbide, leaving the microcutting and pitting the worn surface. Therefore, the main abrasive wear mechanism is microcutting, and submechanism is micropitting. Because the main mechanism occurred on the matrix, the reduction CVF after 3 wt.% Mo makes the higher material loss than 1Mo in the case of 26Cr. However, the wear resistance of high MWCI must be influenced more by the lowering matrix hardness and fracture toughness of M_7C_3 carbide rather than CVF. It can be stated that the solubility of C and the size of M_7C_3 carbide should be controlled rather than only transition metals.

Normally, the surface of metals will experience oxidation phenomenon during the test because of the friction. However, it did not significantly occur on test pieces of this study, which can be evidenced by only a small peak of oxygen detected by

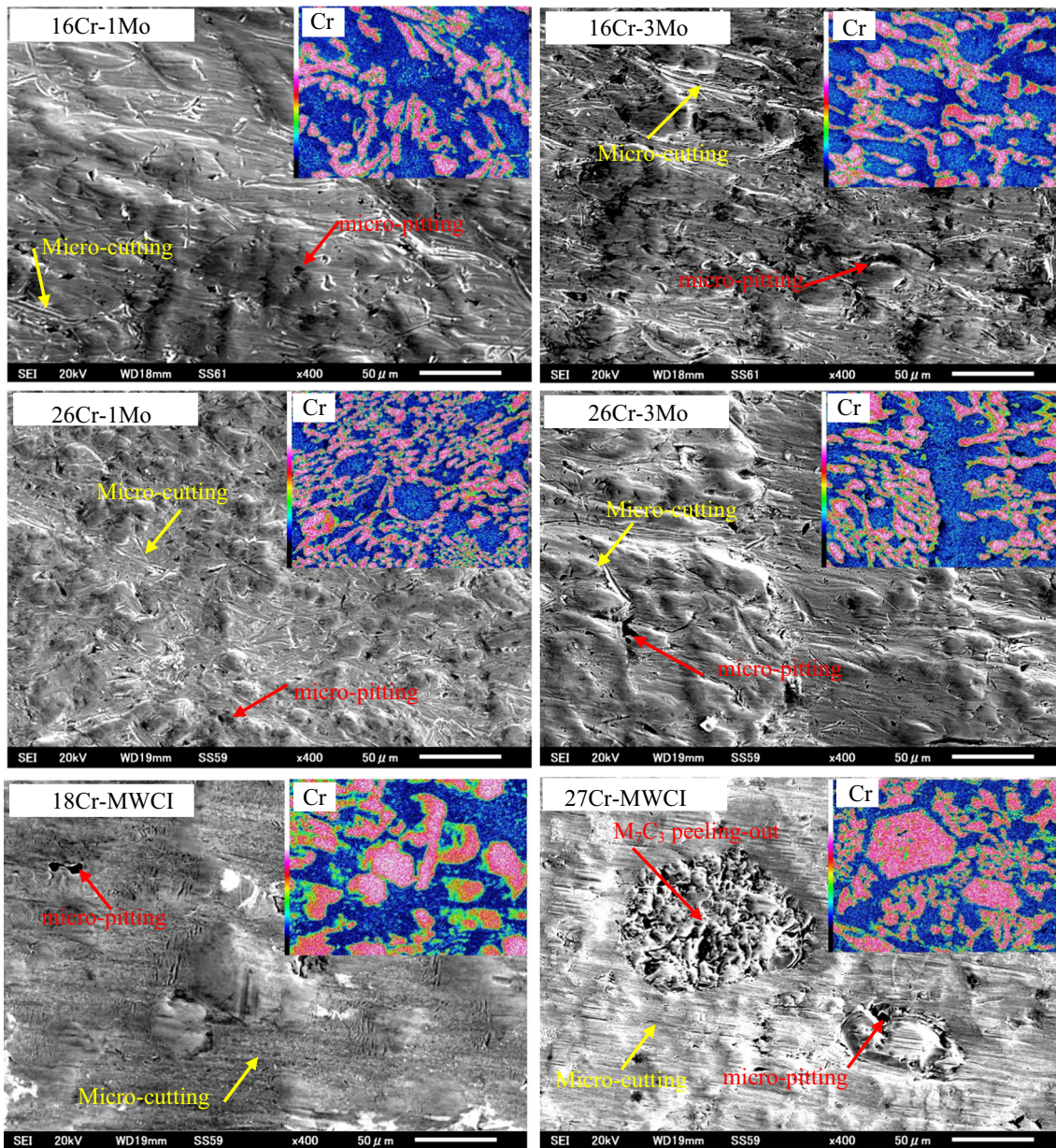


Fig. 11 SEM-EDS microphotograph of materials worn surface after abrasive test

the SEM-EDS, as shown in Fig. 12. Based on a previous study (Ref 9), it has been known that transition metals, especially Cr, have good high-temperature oxidation resistance. This characteristic might make the peak of oxygen difficult to detect on material surfaces after the test. Therefore, the oxidation formation effect during the test can be ignored in this present study. In addition, the profile and depth of the worn material surface are also investigated using laser technology. The result shows the area of grooving on the profile image (Fig. 13) of representative test pieces, which indicates the zone of the three-body abrasive wear. From the depth of the abraded surface (Fig. 14), it can be known that the 16Cr has the deepest, whereas the 18Cr MWCI has the shallower one. This result is consistent with the wear performance of each material.

The observation was continued on the cross section of the most abraded surface as displayed in Fig. 15. The better condition belongs to the higher amount of Mo in the case of

high-Cr-Mo specimens. Besides that, the cross sections of these materials seem more severe than 18Cr MWCI, but a significant difference cannot be observed when compared with 27Cr MWCI. The directly peeling out M_7C_3 carbide on the cross section of 27Cr MWCI can be also clearly observed that must worsen the wear resistance of material. It can be associated with no big difference in abrasive wear resistance between 27Cr MWCI and 26Cr-1Mo as described earlier. With higher magnification as shown in Fig. 16, the plastic deformation of matrix can be observed on the cross section of high-Cr-Mo specimens, which disappears as the amounts of Mo and Cr increase. However, the plastic deformation is difficult to observe in the case of 18Cr and 27Cr MWCI. The existence of the plastic deformation might be influenced by the lower matrix hardness or higher amount of RA. In addition, the M_7C_3 carbide cracking beneath the worn surface can also be seen on all specimens. It can be understood that when the abrasive

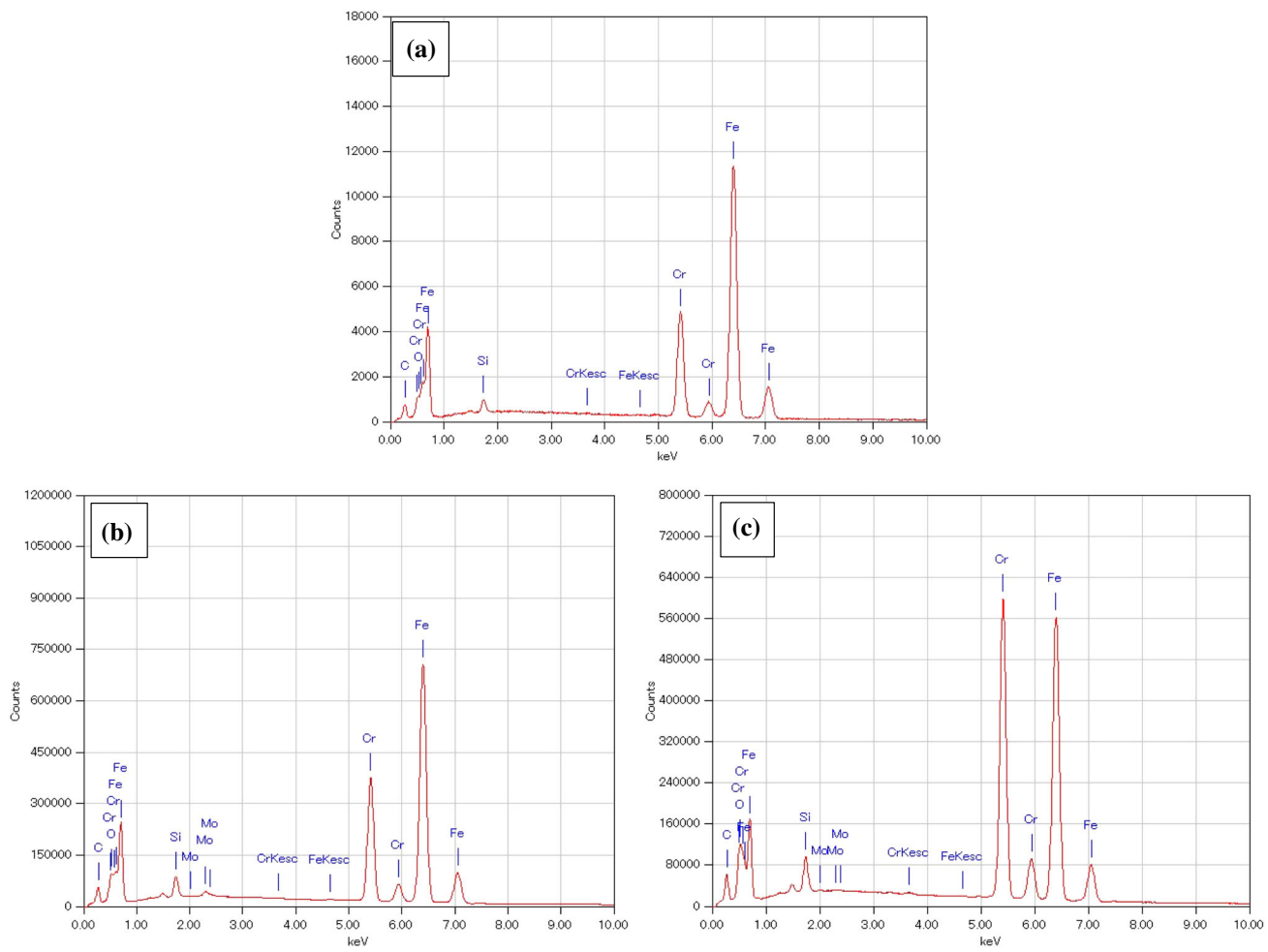


Fig. 12 The surface elemental peak diagram after three-body abrasive wear test of: (a) 16Cr; (b) 16Cr-1Mo; (c) 16Cr-3Mo as the representative materials

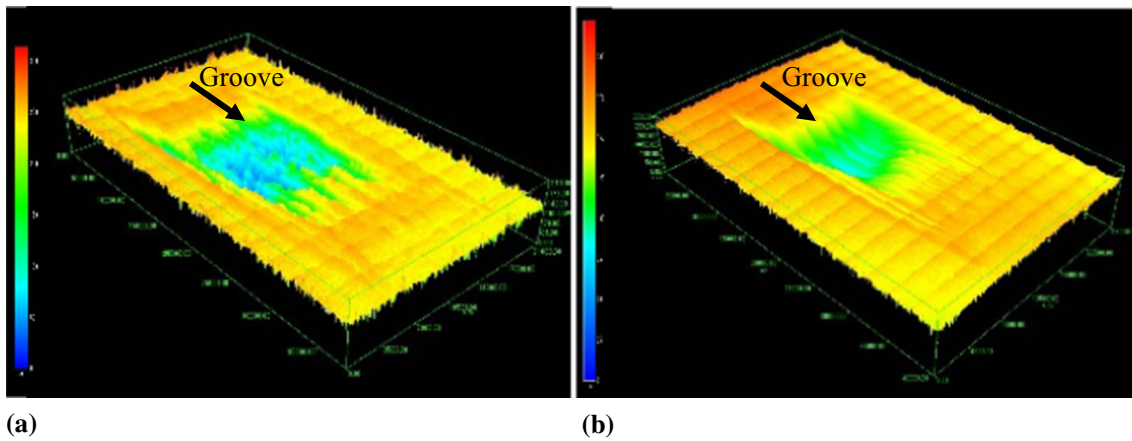


Fig. 13 Mapping of the representative material's surface of (a) 16Cr-1Mo; (b) 27Cr MWCI obtained by laser tech

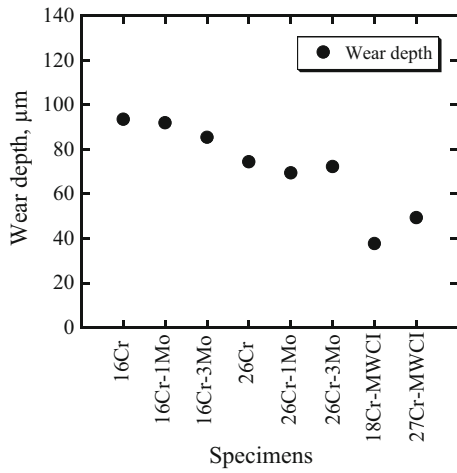


Fig. 14 Worn surface depth of each specimen after test at 196 N applied load

particles hit the material surface, the soft phase (matrix) will experience plastic deformation and push the hard-phase resulting cracking in carbide. Therefore, the higher matrix hardness will reduce the tendency of plastic deformation and carbide cracking leading to better wear resistance. However,

M_7C_3 carbide of 27Cr-MWCI is easily to crack and peel-out that worsens its wear resistance even though the plastic deformation is difficult observed. This carbide is easy to crack may be due to its too large size which has lower toughness or too brittle (Ref 30). The good collaboration among carbon concentrations, the size of M_7C_3 carbide, and the CVF on 18Cr MWCI provides the best abrasive wear resistance among other specimens.

4. Conclusions

All the findings can be concluded that Mo and Cr can significantly increase the CVF, hardness, and wear resistance of HCCI, although the opposite result occurs when Mo addition exceeds 1% wt. in case of 26Cr because of lowering CVF. The wear resistance of 26Cr-1Mo (as the better one among current materials) is only 15% lower than 27Cr MWCI, and it is approximately 53% lower than 18Cr MWCI because of the reduction in the matrix hardness as Cr increases in both comparable materials. Besides that, the larger M_7C_3 carbide on 27Cr MWCI easily peels out owing to brittleness that worsens its wear resistance. Therefore, the three-body abrasive wear characteristics of materials strongly depend on chemical composition, matrix, size of M_7C_3 , and CVF.

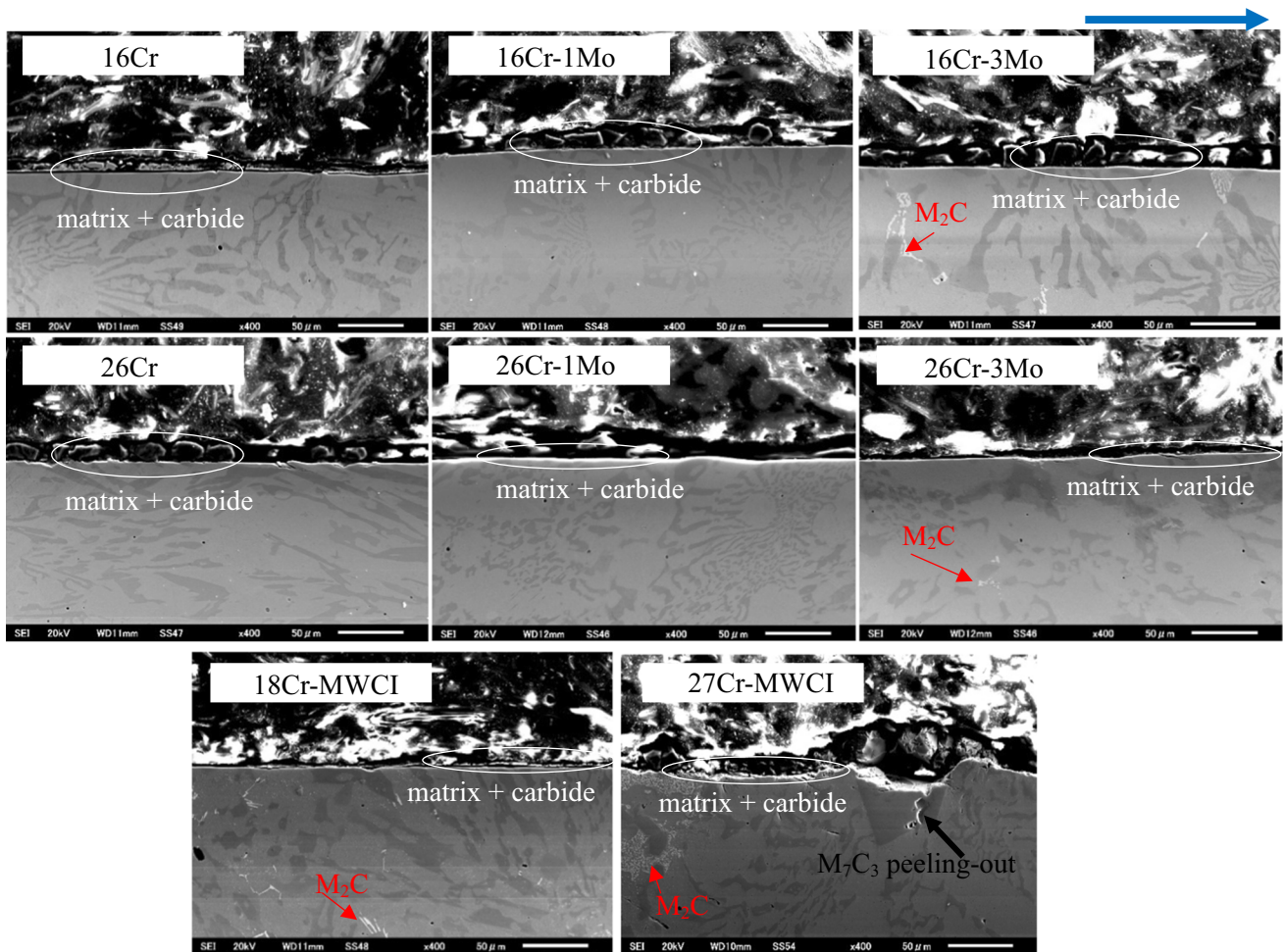


Fig. 15 The cross-sectional observation of the most abraded materials surface. The blue arrow indicates the direction of abrasive wear (Color figure online)

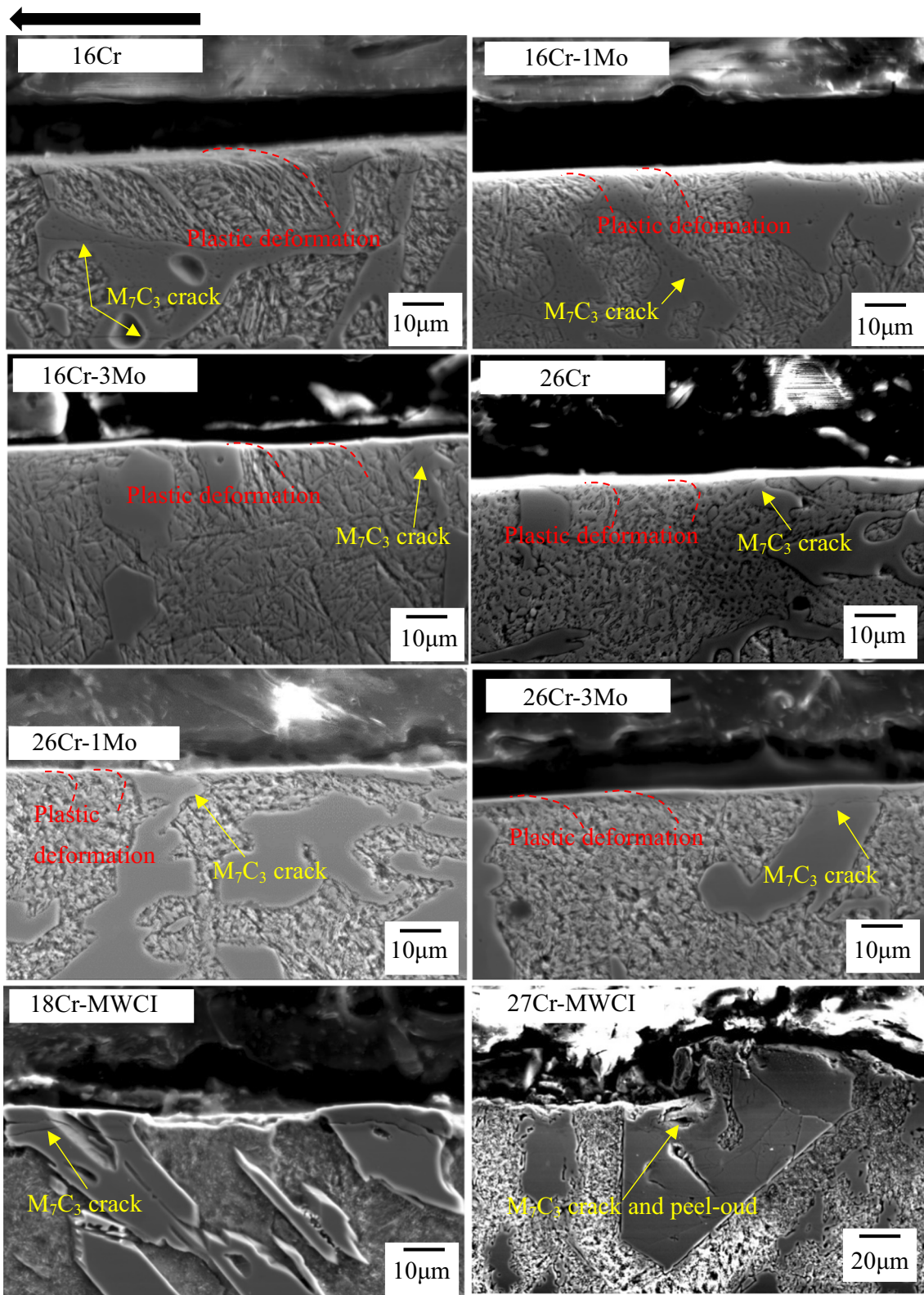


Fig. 16 Plastic deformation and carbide cracking observation with higher magnification on SEM

Conflict of interest

The authors declare that they have no conflicts of interest.

References

1. J. H. Tylczak, *Abrasive Wear ASM Handbook*. (ASM International, 1992)
2. K. Holmberg and A. Erdemir, Influence of Tribology on Global Consumption, Costs, and Emissions, *Friction*, 2017, **5**, p 263–284. <https://doi.org/10.1007/s40544-017-0183-5>
3. P. Kenneth Holmberg, P. Kivikyto-Reponen, K. Harkisaari, and A. E. Valtonen, Global Energy Consumption Due to Friction and Wear in the Mining Industry, *Tribol. Int.*, 2017, **115**, p 116–139.
4. M. Jokari-Sheshdeh, Y. Ali, S.C. Gallo, W. Lin, and J.D. Gates, Comparison the Abrasion Performance of NiHard-4 and High-Cr-Mo White Cast Irons: The Effects of Chemical Composition and Microstructure, *Wear*, 2022, **492–493**, p 204208.
5. O.N. Dogan, J.A. Hawk, and G. Laird II., Solidification Structure and Abrasion Resistance of High Chromium White Cast Irons, *Metall. Mater. Trans. A.*, 1997, **28A**, p 1315–1328.
6. C.P. Tabrett and I.R. Sare, Effect of High Chromium Temperature and Sub Ambient Treatments on the Matrix Structure and Abrasion Resistance of a High Chromium White Iron, *Scripta Mater.*, 1998, **38**(12), p 1747–1753.
7. R.J. Chung, X. Tang, D.Y. Li, B. Hinckley, and K. Dolman, Microstructure Refinement of Hypereutectic High Cr Cast Irons Using Hard Carbide-Forming Elements for Improved Wear Resistance, *Wear*, 2013, **301**, p 695–706.
8. I. Fordyce, M. Annasamy, S.D. Sun, D. Fabijanic, S.C. Gallo, M. Leary, M. Easton, and M. Brandt, The Effect of Heat Treatment on the Abrasive and Erosive Wear Behaviour of Laser Deposited Fe-28Cr-2.7C Alloy, *Wear*, 2020, **458–459**, p 203410.
9. K. Shimizu, R.H. Purba, K. Kusumoto, X. Year, J. Ito, H. Kasuga, and Y. Gaqi, Microstructural Evaluation and High-Temperature Erosion Characteristic of High Chromium Cast Irons, *Wear*, 2019, **426–427**, p 420–427.
10. Y. Li, Ke. Wang, H. Li, M. Gong, and W. Tong, Microstructure and Mechanical Properties of a Mo Alloyed High Chromium Cast Iron after Different Heat Treatments, *Vacuum*, 2018, **156**, p 59–67.
11. H. Gasan and F. Erturk, Effect of Destabilization Heat Treatment on the Microstructure and Abrasive Wear Behavior of High Chromium White Cast Iron Investigated Using Different Characterization Techniques, *Metall. and Mater. Trans. A.*, 2013, **44**, p 4993–5005.
12. A.E. Karantzalis, A. Lakatou and E. Diavati, Effect of Destabilization Heat Treatments on the Microstructure of High Chromium Cast Iron: A Microscopy Examination Approach, *J. Mater. Eng. Perform.*, 2009, **18**, p 1078–1085.
13. T. Todaka, K. Shimizu, K. Kusumoto, R.H. Purba, and Y. Gaqi, Effect Carbon Content on Three-Body Abrasive Wear Characteristics of 28Cr-3Ni Cast Alloys, *ISIJ Int.*, 2021, **61**(8), p 2274–2283.
14. J.J. Coronado, Effect of (Fe, Cr)₇C₃ Carbide Orientation on Abrasion Wear Resistance and Fracture Toughness, *Wear*, 2011, **270**, p 287–293.
15. J. Jiang, S. Li, Hu. Shujun, and Y. Zhou, Effect of In Situ Formed TiC_x on the Microstructure, Mechanical Properties and Abrasive Wear Behavior of High Chromium White Cast Iron, *Mater. Chem. Phys.*, 2018, **214**, p 80–88.
16. H. Pourasiabi and J.D. Gates, Effects of Niobium Macro-Addition to High Chromium White Cast Iron on the Microstructure, Hardness and Abrasive Wear Behaviour, *Mater. Des.*, 2021, **212**, p 110261.
17. K.M. Ibrahim and M.M. Ibrahim, Heat Treatment in High Chromium White Cast Iron Ti Alloy, *J. Metall.*, 2014, **9**, p 1–9.
18. J.J. Penagos, J.I. Pereira, P.C. Machado, E. Albertin, and A. Sinatora, Synergetic Effect of Niobium and Molybdenum on Abrasion Resistance of High Chromium Cast Irons, *Wear*, 2017, **376–377**, p 983–992.
19. A.F. Farah, O.R. Cmkovic, and L.C.F. Canale, Heat Treatment in High Cr White Cast Iron Nb Alloy, *J. Mater. Eng. Perform.*, 2001, **10**, p 42–45.
20. J. Wang, Z. Sun, R. Zuo, C. Li, S.G. Baoluo, and S. Huang, Effect of Secondary Carbide Precipitation and Transformation on Abrasion Resistance of the 16Cr-1Mo-1Cu White Iron, *J. Mater. Eng. Perform.*, 2006, **15**, p 316–319.
21. K.M. Ibrahim and A.A. Nofal, Effect of Titanium Addition on Structure and Properties of the as-Cast High Cr-Mo White Iron, *Int. J. Mater. Res.*, 2013, **103**(3), p 362–370.
22. S. Inthidech, P. Kosasu, S. Yotee, and Y. Matsubara, Effect of Repeated Tempering on Abrasive Wear Behavior of Hypoeutectic 16 Mass% Cr Cast Iron with Molybdenum, *Mater. Trans.*, 2013, **54**, p 28–35.
23. K. Shimizu, K. Kusumoto, X. Yaer, Y. Zhang, and M. Shirai, Effect of Mo Content on Erosive Wear Characteristics of High Chromium Cast Iron at 1173 K, *Wear*, 2017, **376–377**, p 542–548.
24. E. Cortes-Carrilo, A. Bedolla-Jacuinde, I. Mejia, C.M. Zepeda, J. Zuno-Silva, and F.V. Guerra-Lopez, Effect of Tungsten on the Microstructure and on the Abrasive Wear Behavior of a High Chromium White Iron, *Wear*, 2017, **376–377**, p 77–85.
25. D. Kopycinski and S. Piasny, Influence of Tungsten and Titanium on the Structure of High Chromium Cast Iron, *Arch. Foundry Eng.*, 2012, **12**(1), p 57–60.
26. J.D.B. de Mello and A.A. Polycarpou, Abrasive Wear Mechanisms of Multi Component Ferrous Alloys Abraded by Soft, Fine Abrasive Particles, *Wear*, 2010, **269**, p 911–920.
27. S. Inthidech, J. Opapaibon, K. Yamamoto, and Y. Matsubara, Three-Body-Type Abrasive Wear Behavior of Multi-Alloyed White Cast Iron with Different Carbon Contents Used for Hot Work Rolls, *ISIJ Int.*, 2021, **11**, p 2832–2843.
28. K. Kusumoto, K. Shimizu, X. Yaer, Y. Zhang, Y. Ota, and J. Ito, Abrasive Wear Characteristics of Fe-2C-5Cr-5Mo-5W-5Nb Multi-Component White Cast Iron, *Wear*, 2017, **376–377**, p 22–29.
29. K. Kusumoto, K. Shimizu, X. Yaer, H. Hara, K. Tamura, and H. Kawai, High Erosion-Oxidation Performance of Fe-Based Nb or V Containing Multi-Component Alloys with Co Addition at 1173 K, *Mater. Des.*, 2015, **88**, p 366–374.
30. R.H. Purba, K. Shimizu, K. Kusumoto, T. Todaka, M. Shirai, H. Hara, and J. Ito, Erosive Wear Characteristics of High-Chromium Based Multi-Component White Cast Irons, *Tribol. Int.*, 2021, **159**, p 106982.
31. G.L.F. Powell, Structure, Nucleation, Growth and Morphology of Secondary Carbides in High Chromium and Cr-Ni White Cast Irons, *J. Mater. Sci.*, 1992, **27**, p 29–35.
32. K. Kishore, U. Kumar, N. Dinesh, and M. Adhikary, Effect of Soaking Temperature on Carbide Precipitation, Hardness, and Wear Resistance of High-Chromium White Cast Iron, *J. Fail. Anal. Prev.*, 2020, **20**, p 249–260.
33. S.K. Yu, N. Sasaguri and Y. Matsubara, Effects of Retained Austenite on Abrasion Wear Resistance and Hardness of Hypoeutectic High Cr White Cast Iron, *Int. J. Cast Met. Res.*, 1999, **11**, p 561–566.
34. S. Inthidech and Y. Matsubara, Abrasive Wear Resistance of Hypoeutectic 16 wt.% and 26 wt.% Cr Cast Irons with Molybdenum, *Maharakham Int. J. Eng. Technol.*, 2015, **1**(2), p 1–9.
35. J. Sun and Yu. Hao, Microstructure Development and Mechanical Properties of Quenching and Partitioning (Q&P) Steel and an Incorporation of Hot-Dipping Galvanization during Q&P Process, *Mater. Sci. Eng. A.*, 2013, **586**, p 100–107.
36. S. Ma, J. Xing, Y. He, Y. Li, Z. Huang, G. Liu, and Q. Geng, Microstructure and Crystallography of M₇C₃ Carbide in High Chromium Cast Iron, *Mater. Chem. Phys.*, 2015, **161**, p 65–73.
37. S. Liu, Y. Zhou, X. Xing, J. Wang, Y. Yang, and Q. Yang, Agglomeration Model of (Fe, Cr)₇C₃ Carbide in Hypereutectic Fe-Cr-C Alloy, *Mater. Lett.*, 2016, **183**, p 272–276.
38. B. Geng, Y. Li, R. Zhou, Q. Wang, and Y. Jiang, Formation Mechanism of Stacking Faults and its Effect on Hardness in M₇C₃ Carbides, *Mater. Charact.*, 2020, **170**, p 110691.
39. G. Laird, R. Gundlach, and K. Rohrig, *Abrasion-resistant cast iron handbook*, AFS, USA, 2000
40. Y.P. Wang, D.Y. Li, I. Parent, and H. Tian, Improving the Wear Resistance of White Cast Iron Using a New Concept - High-Entropy Microstructure, *Wear*, 2011, **271**, p 1623–1628.
41. M.M. Atabaki, S. Jafari, and H. Abdollah-pour, Abrasive Wear Behavior of High Chromium Cast Iron and Hadfield Steel-a Comparison, *J. Iron Steel Res. Int.*, 2012, **19**, p 43–50.

Publisher's Note Springer Nature remains neutral with regard to jurisdictional claims in published maps and institutional affiliations.